0022-3565/11/3383-906–916$25.00
THE JOURNAL OF PHARMACOLOGY AND EXPERIMENTAL THERAPEUTICS
JPET 338:906–916, 2011

Vol. 338, No. 3
176701/3708757
*Printed in U.S.A.*

# Neuroprotective Efficacy from a Lipophilic Redox-Modulating Mn(III) *N*-Hexylpyridylporphyrin, MnTnHex-2-PyP: Rodent Models of Ischemic Stroke and Subarachnoid Hemorrhage

Huaxin Sheng, Ivan Spasojevic, Hubert M. Tse, Jin Yong Jung, Jun Hong, Zhiquan Zhang, Jon D. Piganelli, Ines Batinic-Haberle, and David S. Warner

*Multidisciplinary Neuroprotection Laboratories (H.S., J.Y.J., D.S.W.), Departments of Anesthesiology (H.S., J.Y.J., Z.Z., D.S.W.), Medicine (I.B.-H.), and Radiation Oncology (I.S.), Duke University Medical Center, Durham, North Carolina; Department of Pediatrics, University of Pittsburgh, Pittsburgh, Pennsylvania (H.M.T., J.D.P.); and Department of Neurosurgery, Tangshan Gongren Hospital, Tangshan Hebei, China (J.H.)*

Received November 7, 2010; accepted June 3, 2011

**ABSTRACT**

Intracerebroventricular treatment with redox-regulating Mn(III) *N*-hexylpyridylporphyrin (MnPorphyrin) is remarkably efficacious in experimental central nervous system (CNS) injury. Clinical development has been arrested because of poor blood-brain barrier penetration. Mn(III) *meso*-tetrakis (*N*-hexylpyridinium-2-yl) porphyrin (MnTnHex-2-PyP) was synthesized to include four six-carbon (hexyl) side chains on the core MnPorphyrin structure. This has been shown to increase in vitro lipophilicity 13,500-fold relative to the hydrophilic ethyl analog Mn(III) *meso*-tetrakis(*N*-ethylpyridinium-2-yl)porphyrin (MnTE-2-PyP). In normal mice, we found brain MnTnHex-2-PyP accumulation to be ~9-fold greater than MnTE-2-PyP 24 h after a single intraperitoneal dose. We then evaluated MnTnHex-2-PyP efficacy in outcome-oriented models of focal cerebral ischemia and subarachnoid hemorrhage. For focal ischemia, rats underwent 90-min middle cerebral artery occlusion. Parenteral MnTnHex-2-PyP treatment began 5 min or 6 h after reperfusion onset and continued for 7 days. Neurologic function was improved with both early ($P = 0.002$) and delayed ($P = 0.002$) treatment onset. Total infarct size was decreased with both early ($P = 0.03$) and delayed ($P = 0.01$) treatment. MnTnHex-2-PyP attenuated nuclear factor $\kappa$B nuclear DNA binding activity and suppressed tumor necrosis factor-$\alpha$ and interleukin-6 expression. For subarachnoid hemorrhage, mice underwent perforation of the anterior cerebral artery and were treated with intraperitoneal MnTnHex-2-PyP or vehicle for 3 days. Neurologic function was improved ($P = 0.02$), and vasoconstriction of the anterior cerebral ($P = 0.0005$), middle cerebral ($P = 0.003$), and internal carotid ($P = 0.015$) arteries was decreased by MnTnHex-2-PyP. Side-chain elongation preserved MnPorphyrin redox activity, but improved CNS bioavailability sufficient to cause improved outcome from acute CNS injury, despite delay in parenteral treatment onset of up to 6 h. This advance now allows consideration of MnPorphyrins for treatment of cerebrovascular disease.

## Introduction

Oxidative stress is a component of ischemic brain injury (Warner et al., 2004; Niizuma et al., 2009). Efforts to pharmacologically improve outcome from focal cerebral ischemia have focused largely on antioxidants not offering catalytic activity (i.e., scavengers). Although frequently found efficacious in preclinical studies (Hall et al., 1990; Marshall et al., 2003), scavengers have not translated into positive human trials (The RANTTAS Investigators, 1996; Shuaib et al., 2007).

Redox-regulating catalytic antioxidants, such as pentacationic Mn(III) *N*-alkylpyridylporphyrins (MnPorphyrins; charges omitted throughout text for clarity) exert remarkable in vivo antioxidant potency (Batinić-Haberle et al., 2010a,b). Their

This work was supported by, in part, by the National Institutes of Health National Center for Research Resources [Clinical and Translational Science Award 1 UL1 RR-024128–01] (to D.S.W., I.B.H., H.S., and I.S.).
Article, publication date, and citation information can be found at http://jpet.aspetjournals.org.
doi:10.1124/jpet.110.176701.

**ABBREVIATIONS:** MnPorphyrin, Mn(III) *N*-alkylpyridylporphyrin; SOD, superoxide dismutase; ACA, anterior cerebral artery; BBB, blood-brain barrier; CNS, central nervous system; ICA, internal carotid artery; IL-6, interleukin-6; LDF, laser Doppler flow; MAP, mean arterial pressure; MCA, middle cerebral artery; MCAO, MCA occlusion; NF-$\kappa$B, nuclear factor $\kappa$B; $PaCO_2$, partial pressure of carbon dioxide; $PaO_2$, partial pressure of oxygen; PBS, phosphate-buffered saline; ROI, region of interest; SAH, subarachnoid hemorrhage; TNF-$\alpha$, tumor necrosis factor-$\alpha$; MnTE-2-PyP, Mn(III) *meso*-tetrakis(*N*-ethylpyridinium-2-yl)porphyrin; MnTnHex-2-PyP, Mn(III) *meso*-tetrakis (*N*-hexylpyridinium-2-yl) porphyrin; MnTDE-2-ImP, Mn(III) *N,N′*-dialkylimidazolyl porphyrin; MnTBAP, Mn(III) tetrakis (4-benzoic acid)porphyrin chloride; DTT, dithiothreitol; PMSF, phenylmethylsulfonyl fluoride.

potency is based on the positive charges placed on the *meso* pyridyl rings in the *ortho* positions close to the Mn center, whereby both strong electron-withdrawing and electrostatic effects are exerted (Batinić-Haberle et al., 1998). Consequently, such MnPorphyrins possess a favorable metal-centered reduction potential, $E_{1/2}$ for Mn(III)P/Mn(II)P redox couple, while their penta-cationic charge attracts anionic superoxide ($O_2^{\cdot-}$) and peroxynitrite to the Mn site. The same is true for the endogenous superoxide dismutase (SOD) enzymes these compounds mimic. Thus, both favorable thermodynamics ($E_{1/2}$) and kinetics (charges) for $O_2^{\cdot-}$ dismutation, catalyzed by SOD enzymes, result in the diffusion-limited $k_{cat}$ ($O_2^{\cdot-}$) of $\sim 10^9\ M^{-1} \cdot s^{-1}$. The most potent MnPorphyrin compounds have $k_{cat}$ nearly identical to the $k_{cat}$ of SOD enzymes (DeFreitas-Silva et al., 2008; Batinić-Haberle et al., 2010a).

Because of the easy reducibility of Mn(III)P to Mn(II)P with ascorbate and GSH, the removal of $O_2^{\cdot-}$ and peroxynitrite by MnPorphyrins is probably coupled with these abundant cellular reductants (Batinić-Haberle et al., 2010b). In the first step of the dismutation process, Mn(III)P would be reduced to Mn(II)P with ascorbate or glutathione (accepting electron from either reductant). In a subsequent step, Mn(II)P would be oxidized with $O_2^{\cdot-}$ closing the catalytic cycle. In this scenario, MnPorphyrins would mimic superoxide reductase (that some organisms possess) rather than SOD. Based on the same thermodynamics and kinetics, which are favorable for scavenging $O_2^{\cdot-}$ and peroxynitrite, MnPorphyrins effectively scavenge nitric oxide, carbonate radical, and hypochlorous acid (Spasojevic et al., 2000; Zhang et al., 2002). It is noteworthy that these cationic substituted pyridylporphyrins also modulate redox-regulated activation of transcription factors implicated in inflammatory and immune responses (Spasojevic et al., 2000; Batinić-Haberle et al., 2009a, 2010 a,b, 2011b; Sheng et al., 2009). The prevailing understanding is that MnPorphyrins remove signaling reactive species, which would otherwise activate transcription factors, thereby serving as antioxidants. An alternative and well justified scenario is that MnPorphyrins oxidize p50 or glutathionylate p65 subunits of NF-κB (in the presence of glutathione and $H_2O_2$), thereby acting as pro-oxidants (Tse et al., 2004; Batinić-Haberle et al., 2010b, 2011a,b; Jaramillo et al., 2010).

These compounds have been evaluated in both mouse and rat models of middle cerebral artery occlusion (MCAO). Cationic *ortho* Mn(III) *N*-alkylpyridyl- and *N,N′*-dialkylimidazolyl porphyrins such as MnTE-2-PyP and MnTDE-2-ImP, respectively, have repeatedly been found efficacious (Mackensen et al., 2001; Sheng et al., 2002b, 2009). However, both molecules carry a net 5+ charge, which markedly limits BBB and cell membrane penetration. This would be expected to attenuate brain entry and bioavailability and therefore decrease potency (Batinić-Haberle et al., 2009b). Consequently, intracerebroventricular injection/infusion has been required to demonstrate sustained efficacy in the rat (Sheng et al., 2009). Short-term MCAO outcome studies with the hydrophilic ethyl analog MnTE-2-PyP have shown efficacy when given intravenously (Mackensen et al., 2001; Sheng et al., 2002b, 2009). However, doses near the toxic threshold were required to obtain efficacy. In contrast, MnTnHex-2-PyP offers structural properties consistent with markedly enhanced lipophilicity caused by the substitution of ethyl with hexylpyridyl chains while retaining the crucial positive charges close to the metal center (Kos et al., 2009). Figure 1 shows those two Mn(III) *N*-alkylpyridylporphyrins, where alkyl chains are ethyl groups in the case of MnTE-2-PyP and hexyl groups in the case of MnTnHex-2-PyP. The four alkyl groups are placed close to the porphyrin meso bridges on *ortho* pyridyl nitrogens. The difference in the length of alkyl groups confers a 13,500-fold higher lipophilicity of the hexyl versus ethyl analog (Batinić-Haberle et al., 2011b). Also shown is the imidazolium analog, MnTDE-2-ImP$^{5+}$ (AEOL10150), which has eight ethyl groups on both *ortho* nitrogens of meso imidazolium substituents, and whose positive charges are delocalized over the imidazolium rings rather than being placed on

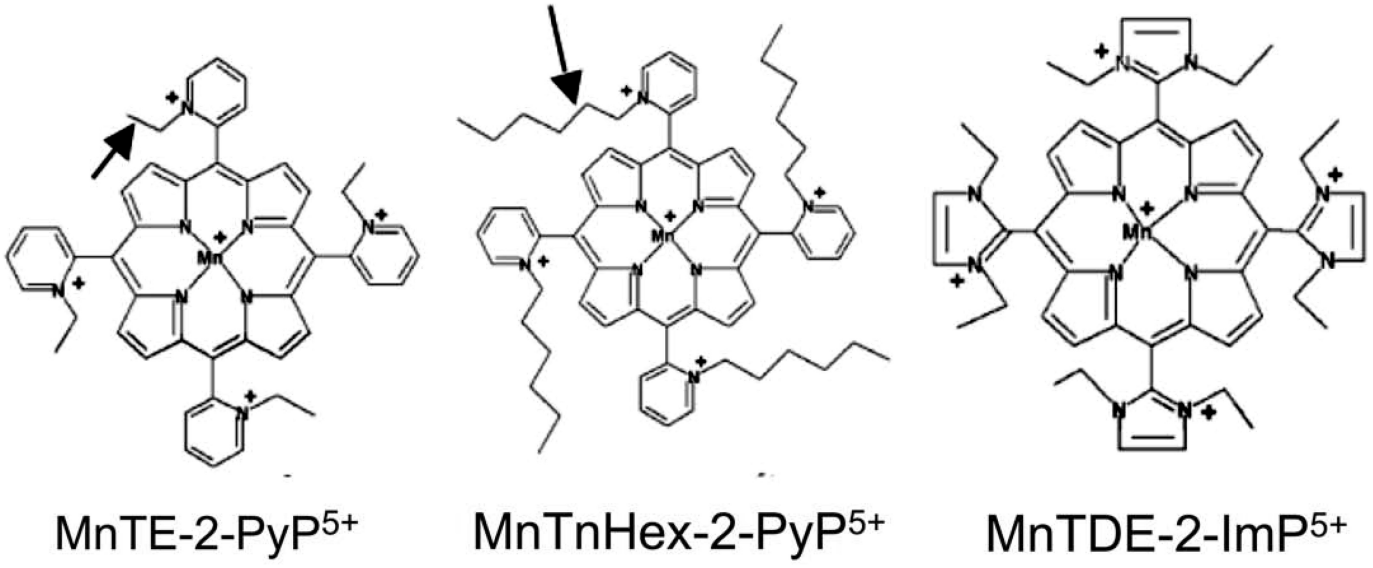


**Fig. 1.** Structural formulas for three MnPorphyrins evaluated to date in rodent middle cerebral artery occlusion models. Note the ethyl and hexyl side chains on *ortho* alkylpyridylporphyrins, MnTE-2-PyP$^{5+}$ (AEOL10113) and MnTnHex-2-PyP$^{5+}$ (arrows). The hexyl extension causes markedly increased lipophilicity and blood-brain barrier penetration without substantive changes in redox activity (Table 1). The di*ortho*-alkylimidazolylporphyrin, MnTDE-2-ImP$^{5+}$ (AEOL10150) is also shown. Compared with pyridyl analogs, MnTE-2-PyP$^{5+}$ and MnTnHex-2-PyP$^{5+}$, MnTDE-2-ImP$^{5+}$ has two ethyl groups on two nitrogens of each imidazolium meso substituent.

one of two nitrogens. The molecule is thus bulkier, which has affected its transport across the *Escherichia coli* cell wall (Batinić-Haberle et al., 2011b). For the same reason, however, the positive charges are less exposed to biological targets, which might have been the cause of lower toxicity, as seen in in vivo studies (Sheng et al., 2002a).

This series of experiments offers the first examination of the lipophilic MnTnHex-2-PyP in the context of acute central nervous system (CNS) injury. We hypothesized that the hexyl substitution would improve outcome in experimental focal cerebral ischemia and subarachnoid hemorrhage when given parenterally. We also report data relevant to the effects of MnTnHex-2-PyP on BBB penetration, ischemia-induced NF-κB nuclear DNA binding, and subsequent cytokine expression.

## Materials and Methods

The following studies were approved by the Duke University Animal Care and Use Committee.

**Experiment 1: MnTnHex-2-PyP Pharmacokinetics.** MnTnHex-2-PyP was synthesized as described previously (Batinić-Haberle et al., 2002). Two kinetic studies were performed. Naive male Wistar rats (250–275 g; Harlan, Indianapolis, IN) were anesthetized with isoflurane, and a jugular venous catheter was placed. The rats were simultaneously given MnTnHex-2-PyP at 75 μg/kg i.v. and 225 μg/kg s.c. The catheter was removed, and the rats were allowed to awaken. The subcutaneous dose was repeated every 12 h for 7 days. At 1 h, 4 h, 1 day, 3 days, or 7 days after treatment onset the rats were anesthetized and blood was sampled (on days 1, 3, and 7, blood was sampled 4 h after the final dose). Immediately after blood sampling, the vasculature was rinsed in situ with 0.9% NaCl, and the brains were harvested. Plasma and brain MnTnHex-2-PyP concentrations were measured (four rats per time point) using established liquid chromatography/mass spectrometry methods (Spasojevic et al., 2011; Batinić-Haberle et al., 2011b).

Because the effects of sustained treatment with MnTnHex-2-PyP in the rat are unknown, we took additional measures on the rats destined for 7-day survival. Body weight was measured before the first injection and after completion of the 7-day treatment regimen. In addition, these rats underwent evaluation of rotarod performance. Before the first MnTnHex-2-PyP injection, rats were tested three times on an accelerating rotarod (4–40 rpm), with 15-min intertrial resting intervals. The latency to fall was recorded with a maximum testing interval of 500 s. Rotarod performance was repeated on day 7, before euthanasia. The best performance score among the three trials for each animal was compared with baseline values.

In a second experiment, three naive C57BL/6J mice were given a single intraperitoneal injection of MnTnHex-2-PyP (2 mg/kg). Brain MnTnHex-2-PyP concentrations were measured 24 h later as described above. Values were compared with those previously obtained using an identical protocol in mice given 10 mg/kg i.p. MnTE-2-PyP (Spasojevic et al., 2008b).

**Experiment 2: Dose Finding Studies.** MnPorphyrins elicit known arterial hypotension responses unique to the rat, which are absent in other species (including mouse, dog, and baboon), plausibly because of the unique dimeric extracellular superoxide dismutase structure in the rat (Ross et al., 2002). Because arterial hypotension could confound brain perfusion and thus MCAO outcome, we conducted a dose escalation study to define the maximal MnTnHex-2-PyP dose tolerated so as to not cause a sustained change in blood pressure recorded at 5-min intervals over 60 min. We examined an intravenous injection of 75, 225, and 450 μg/kg MnTnHex-2-PyP given over 5 min in separate rat cohorts ($n$ = 1–3).

**Experiment 3: 90-Minute MCAO, Treatment Onset 5 Min after Reperfusion Onset.** Male Wistar rats (10–12 weeks of age; Harlan) were allowed access to water but fasted from food for 12 h to standardize the glycemic state. Rats were then anesthetized with isoflurane in $O_2$. After orotracheal intubation, the lungs were mechanically ventilated to maintain normocapnia. A 22-gauge needle thermistor was percutaneously placed adjacent to the skull beneath the temporalis. Pericranial temperature was servoregulated at 37.5 ± 0.1°C by surface heating or cooling. The inspired isoflurane concentration was adjusted to 1.0 to 1.5% in 50% $O_2$/balance $N_2$. The tail artery was cannulated. The animals were then prepared for MCAO as described previously (Longa et al., 1989; Mackensen et al., 2001). Via a midline cervical incision the right common carotid artery was identified. The external carotid artery was isolated, and the occipital, superior thyroid, and external maxillary arteries were ligated and divided. The internal carotid artery (ICA) was dissected distally until the origin of the pterygopalatine artery was visualized. After surgical preparation, a 20-min interval was allowed for physiologic stabilization.

Five minutes before MCAO onset, heparin (50 IU intra-arterial) was given to prevent intra-arterial thrombosis. The common carotid artery was temporarily occluded. A 0.25-mm-diameter nylon monofilament (distal 5-mm tip coated with 0.38-mm-diameter silicone) was inserted into the external carotid artery stump and passed distally through the ICA (approximately 20 mm from carotid bifurcation) until a slight resistance was felt and the filament was secured. At MCAO onset, isoflurane was reduced to 0.8 to 1.0%.

After 90-min MCAO, the filament was removed and the common carotid artery was deoccluded. Five minutes later, rats were randomly allocated to treatment groups. Vehicle [0.3 ml of phosphate-buffered saline (PBS)] or MnTnHex-2-PyP 225 μg/kg (0.3 ml) was injected over 5 min into the internal jugular vein ($n$ = 18 per group). Thirty minutes later, this was followed by either subcutaneous 0.3 ml of PBS or 225 μg/kg MnTnHex-2-PyP, respectively. The anesthetic state and pericranial temperature regulation were continued for an additional 100 min to standardize early reperfusion physiology. The tail artery catheter was then removed. The wounds were infiltrated with bupivacaine and closed with suture. Isoflurane was discontinued. Upon recovery of the righting reflex, the tracheas were extubated. The animals were placed in an $O_2$-enriched environment (fraction of inspired oxygen = 30%) for 1 h and then returned to their cages.

At 10 h after MCAO, PBS or 225 μg/kg MnTnHex-2-PyP was given subcutaneously. This was repeated twice daily for the next 6 days. Our decision to study sustained treatment with MnTnHex-2-PyP was based on prior work that showed MnPorphyrins provide enduring efficacy only when treatment duration is continued for up to 1 week (Sheng et al., 2009).

Seven days after MCAO, rats were subjected to a previously described standardized neurologic evaluation (Yokoo et al., 2004; Sakai et al., 2007). The neurological scoring system evaluated four different functions (general status, simple motor deficit, complex motor deficit, and sensory deficit). The score given to each animal (by an observer blinded to group assignment) was the sum of all four individual scores, 0 being the minimum (best) score and 48 being the maximum (worst) score. This scoring system has been shown to correlate well with cerebral infarct size (Yokoo et al., 2004).

The animals were then weighed, anesthetized with isoflurane, and decapitated. The brains were removed, frozen at −40°C in 2-methylbutane, and stored at −70°C. Serial quadruplicate 20-μm-thick coronal sections were taken using a cryotome at 660-μm intervals over the rostral-caudal extent of the infarct. The sections were dried and stained with hematoxylin and eosin. A section from each 720-μm interval was digitized with a video camera controlled by an image analyzer. The image of each section was stored as a 1280 × 960 pixel matrix and displayed on a video monitor. With the observer blinded to experimental condition, the following regions of interest (ROI) were cursor outlined: noninfarcted ipsilateral cerebral cortex, noninfarcted ipsilateral subcortex, contralateral cerebral cortex, and contralateral subcortex. The area within each ROI ($mm^2$) was deter-

mined by automated counting of calibrated pixels. Ipsilateral noninfarcted cortex and subcortex areas were subtracted from the corresponding contralateral ROI values to estimate the area of ischemic tissue damage (Swanson et al., 1990). Infarct volumes (cubic millimeters) were computed as running sums of subtracted infarct area multiplied by the known interval (e.g., 800 μm) between sections over the rostral-caudal extent of the infarct calculated as an orthogonal projection (Warner et al., 1995).

**Experiment 4: 90-Min MCAO, Treatment Onset 6 h after Reperfusion Onset.** Rats were subjected to the same anesthesia, surgical preparation, and MCAO insult as in experiment 3. The tail artery catheter was secured against dislodgement and left in place after emergence from anesthesia. At 6 h after reperfusion (7.5 h after MCAO onset), rats were randomly assigned to two groups: vehicle ($n = 10$) and MnTnHex-2-PyP ($n = 9$).

For the vehicle group, 0.3 ml of PBS was injected into the tail artery to avoid requirement for additional vascular access in the conscious animal. A subcutaneous injection of PBS (0.3 ml) was made at the same time and repeated twice daily.

For the MnTnHex-2-PyP group, 225 μg/kg MnTnHex-2-PyP was injected into the tail artery over 5 min. A subcutaneous injection of 225 μg/ml MnTnHex-2-PyP (0.3 ml) was given at the same time and repeated twice daily.

At completion of the 7-day recovery interval, rats were subjected to neurologic evaluation and measurement of cerebral infarct volume as described for experiment 1.

**Experiment 5: 90-Min MCAO, Treatment Onset 6 h after Reperfusion Onset/Validation with Laser Doppler Flowmetry.** The primary purpose of this study was to assure that there were no intraischemic differences in cerebral blood flow to which improved outcome observed in the MnTnHex-2-PyP group could be attributed. Anesthetic, surgical, and monitoring procedures described for experiment 3 were repeated. Thirty-two rats were subjected to 90-min MCAO. In addition, a midline scalp incision was made for placement of a 3-mm-diameter LDF probe (model BPM2; Vasamedics LLC, Minneapolis, MN) over the ischemic cortex. A 3-mm-diameter burr hole was made through the outer table of the skull over the right hemisphere 5.5 mm lateral to midline and 1.0 mm posterior to bregma, within which the LDF probe was positioned. LDF was continuously measured and recorded at 15-min intervals for 30 min before, during, and for 15 min after MCAO. Incisions were infiltrated with bupivacaine (0.25%), catheters were removed, and wounds were closed with suture. The rats were allowed to awaken. The tracheas were extubated, and the animals were returned to their cages. At 6 h after reperfusion onset, rats were randomly assigned by a computer-generated sequence to either vehicle or MnTnHex-2-PyP treatment doses, using a dosing schedule identical to that used in experiment 4. As above, the animal surgeon was blinded to treatment group, injections were made by another experimenter, and neurologic score and cerebral infarct volume analysis were made by an experimenter blinded to group assignment 7 days after MCAO, as described above.

**Experiment 6: Brain TNF-α and IL-6.** Rats were subjected to MCAO as described above. Five minutes after onset of reperfusion, rats were randomly treated with vehicle ($n = 3$) or 225 μg/kg i.v. MnTnHex-2-PyP ($n = 3$) followed by subcutaneous vehicle or 225 μg/kg MnTnHex-2-PyP, respectively, at 12 and 18 h after MCAO. Twenty-four hours after reperfusion onset, the brains were harvested and the ipsilateral forebrain was excised. Approximately 100 mg of brain tissue was diced on ice, placed into a prechilled microcentrifuge tube containing 300 μl of ice-cold lysis buffer (50 mM Tris-HCl, pH 7.5, 150 mM NaCl, 1% Nonidet P40, 0.5% sodium deoxycholate, 0.1% SDS, and protease inhibitors). Samples were homogenized for 10 s and then incubated for 30 min on ice. Homogenates were centrifuged at 12,000*g* for 10 min at 4°C. Supernatants were collected and proteins concentrations were measured using a BCA Protein Assay Kit (Thermo Fisher Scientific, Waltham, MA) according to the manufacturer's instructions. Cerebral TNF-α and IL-6 concentrations were determined by rat specific enzyme-linked immunosorbent assay kits (Thermo Fisher Scientific) and normalized by the total amount of protein (picograms per milligram).

**Experiment 7: NF-κB Nuclear DNA Binding.** Four rats ($n = 2$ per group) were subjected to 90-min MCAO as described above. Five minutes after reperfusion onset they were randomly allocated to receive either vehicle (PBS) or MnTnHex-2-PyP (225 μg/kg i.v.). Six hours later, the ipsilateral hemisphere was harvested for electromobility-shift assay performed on nuclear extracts (2.5 μg). Tissue was snap-frozen in liquid nitrogen and stored at −80°C for later analysis. After all samples were collected, nuclear protein extraction was performed. The tissue was homogenized in an ice-cold lysis buffer (0.5% Nonidet P40 Substitute, 10 mM HEPES, 1.5 mM $MgCl_2$, 10 mM KCl, 0.5 mM EDTA, 0.5 mM DTT, 0.12 M sucrose, 1 mM PMSF, and 1% protease inhibitor cocktail) using a Dounce homogenizer, incubated on ice for 10 min, and centrifuged at 10,000*g* for 2 min. Nuclear pellets were washed once with lysis buffer without NP40 or sucrose and centrifuged. Supernatants were discarded and nuclear pellets were resuspended in an equal volume of ice-cold buffer containing 20 mM HEPES, 1.5 mM $MgCl_2$, 0.5 mM DTT, 0.6 M KCl, 25% glycerol, 1 mM PMSF, and 1% protease inhibitor, incubated with shaking for 30 min at 4°C, and then centrifuged at 12,000*g* for 20 min at 4°C. The resulting supernatants containing nuclear protein were collected, and the protein concentrations were determined using the Bradford protein reagent (Thermo Fisher Scientific). NF-κB double-stranded consensus oligonucleotide (5′-AGTTGAGGGGACTTTCC CAGGC-3′) was labeled with $^{32}$P-ATP using T4 polynucleotide kinase. In a total volume of 15 μl, purified $^{32}$P-labeled probe was incubated with 5 μg of nuclear protein in a binding reaction mixture containing 10 mM Tris-HCl, pH 7.9, 1 mM EDTA, 50 mM NaCl, 10% glycerol, 0.02% Nonidet P40, 0.2 mM PMSF, 1 mM DTT, and 0.5 μg of poly(dI-dC) for 20 min at room temperature. Bound complex was separated from free probe by electrophoresis through a 60-min prerun 6% nondenaturing acrylamide/bisacrylamide (19:1) gel in 0.5× Tris-borate/EDTA at 150 V. Gels were vacuum-dried, and x-ray autoradiography was performed. The NF-κB bands were analyzed using densitometry. The NF-κB band used to quantify the effect of drug on NF-κB DNA binding was confirmed in tissue extracts by supershift analysis with 1 μg of anti-NF-κB p65 antibody (Santa Cruz Biotechnology, Inc., Santa Cruz, CA) per 5 μg of nuclear protein incubated for 30 min before adding the probe. Specificity of probe binding was confirmed by competition with unlabeled probe (NF-κB consensus oligonucleotide sequence) at a ratio of 100:1.

**Experiment 8: Mouse Subarachnoid Hemorrhage.** Experiments were conducted on male C57BL/6J mice (The Jackson Laboratory, Bar Harbor, ME) weighing between 20 and 25 g, by a surgeon blinded to group assignment. SAH was induced in isoflurane-anesthetized mechanically ventilated mice by endovascular perforation of the anterior cerebral artery (ACA) with pericranial temperature maintained at 37.0 ± 0.2°C (McGirt et al., 2002; Parra et al., 2002; Sheng et al., 2011). After ACA perforation, the mice were awakened.

Mice were then randomly allocated to treatment groups. Intraperitoneal PBS ($n = 15$) or 225 μg/kg MnTnHex-2-Pyp ($n = 15$) was given twice per day for 3 days beginning 60 min after ACA perforation. The recovery interval lasted 72 h. This has been previously defined as the interval of peak vasospasm for this model (Kamii et al., 1999). Mice then underwent a focal neurologic examination identical to that described above for MCAO with the observer blinded to group assignment.

Mice were then anesthetized and standardized casting of the cerebral vasculature was performed using an India Ink/gelatin solution under controlled perfusion pressure (80–100 mm Hg) (McGirt et al., 2002; Parra et al., 2002; Sheng et al., 2011). Hemorrhage area was scored by an observer blinded to group assignment as follows: 1, SAH extends anterior <1.0 mm from the MCA-ACA bifurcation; 2, SAH extends >1.0 mm anterior from the bifurcation; and 3, SAH extends >1.0 mm anterior from the bifurcation with posterior extension across the ICA (Parra et al., 2002). Hemorrhage density was

scored as: 1, underlying brain parenchyma visualized through clot and 2, underlying brain parenchyma not visualized through clot. Hemorrhage grade (2–5) was determined by the sum of the size and density scores. Absence of hemorrhage was scored as 0 (Parra et al., 2002).

Cross-sectional diameters of the right ACA, MCA, ICA, and basilar artery were measured, by an observer blinded to group assignment, using a video-linked dissecting microscope controlled by an image analyzer (Parra et al., 2002). The image of each section was stored as a 1280 × 960 matrix of calibrated pixel units and displayed on a video screen. Two regions of the ipsilateral MCA were analyzed; a 1.0-mm segment proximal to the ACA-MCA bifurcation and a 1.0-mm segment distal to the bifurcation. The ipsilateral ICA and ACA were divided into proximal and distal 0.8-mm segments. The smallest lumen diameter within each vascular segment was measured from the digitized images. Five naive mice were subjected to the same perfusion procedure to provide normal reference values. These mice were not included in the statistical analysis.

To assure that MnTnHex-2-PyP had no effect on blood pressure in mice, as would be predicted from previous work with MnPorphyrins (Ross et al., 2002), four mice were anesthetized with 1.2% isoflurane, and the lungs were mechanically ventilated. A femoral artery was cannulated. MAP was continuously measured and recorded at 5-min epochs for 30 min to establish baseline values. MnTnHex-2-PyP (225 μg/kg) was given intraperitoneally, and MAP was monitored for an additional 60 min.

**Statistical Analysis.** An a priori power analysis was conducted using data from the same model reported in prior studies (Mackensen et al., 2001; Sheng et al., 2002b), which indicated that a group size of 18 rats would be sufficient to allow detection of a 40% reduction in cerebral infarct size after MCAO given $b = 0.8$ and $P < 0.05$. Given the effect size observed in experiment 3, subsequent studies were performed with a decreased sample size to conserve animals. Physiologic values, cerebral infarct volumes, and cytokine concentrations were compared by unpaired Student's $t$ test. For the SAH experiment, cerebral vessel diameters were compared using Student's $t$ test. Hemorrhage grades and neurologic scores (in both models) were compared by the Mann-Whitney U statistic. MAP values in mice subjected to intraperitoneal MnTnHex-2-PyP were compared (preinjection versus 60 min after injection) by the paired Student's $t$ test. LDF was compared between groups by repeated-measures analysis of variance. Total infarct volume was compared with neurologic score using the Spearman rank correlation coefficient. Parametric data are expressed as mean ± S.D. Nonparametric data are expressed as median ± interquartile range.

## Results

**Experiment 1: MnTnHex-2-PyP Pharmacokinetics.** Plasma and brain values from the rat study are presented in Fig. 2. MnTnHex-2-PyP was found to accumulate in brain over the 7-day treatment interval, with brain concentrations at 7 days after treatment onset approaching plasma concentrations. Brain concentrations from mice given a single dose of 2 mg/kg i.p. MnTnHex-2-PyP are included in Table 1. Brain MnTnHex-2-PyP concentrations were similar to those previously reported in mice given 10 mg/kg i.p.MnTE-2-PyP (Spasojevic et al., 2008b). When values were normalized for the 5-fold smaller MnTnHex-2-PyP dose, brain MnTnHex-2-PyP accumulation was calculated to be increased ~9-fold by the hexyl substitution.

Body weight change was not different between vehicle-treated (+30 ± 9 g) versus MnTnHex-2-PyP-treated rats (+38 ± 3 g; $P = 0.14$) over the 7-day treatment interval. Rotarod performance at 7 days (percentage baseline performance) was similar between groups (vehicle = 114 ± 58% versus MnTnHex-2-PyP = 118 ± 56%; $P = 0.95$).

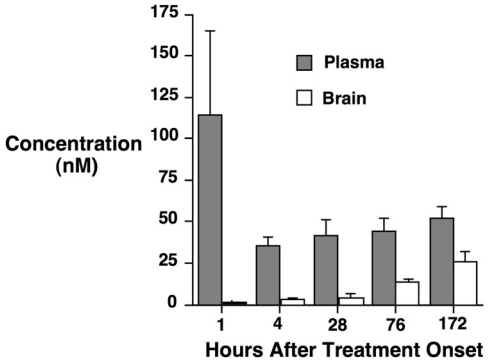


**Fig. 2.** Rats were simultaneously given 75 μg/kg i.v. and 225 μg/kg s.c. MnTnHex-2-PyP. The subcutaneous dose was repeated every 12 h for 7 days. Plasma and brain MnTnHex-2-PyP concentrations were sampled at 1, 4, 28, 76, and 172 h after treatment onset (four rats per time point). For 28, 76, and 172 h, samples were taken 4 h after last injection. Values are mean ± S.D. Progressive brain MnTnHex-2-Pyp accumulation was observed.

**Experiment 2: Dose-Finding Studies.** An intravenous dose of 75 μg/kg MnTnHex-2-PyP caused no change in blood pressure. MnTnHex-2-PyP at 225 μg/kg i.v. decreased MAP to as low as 60 mm Hg for 15 to 20 min after which MAP normalized. An intravenous dose of 450 μg/kg MnTnHex-2-PyP caused profound and sustained MAP reduction. We therefore accepted a bolus dose of 225 μg/kg for subsequent studies, and this dose was emulated as a subcutaneous dose for sustained treatment regimens.

**Experiment 3: 90-Min MCAO, Treatment Onset 5 Min after Reperfusion Onset.** One rat died in the vehicle-treated group. Physiologic values are reported in Table 2. Minor differences were present for preischemic $PaCO_2$ and hematocrit. Rats treated with MnTnHex-2-PyP gained body weight over the 7-day recovery period, whereas rats treated with vehicle lost weight ($P = 0.02$). Median ± interquartile range neurologic scores were improved by MnTnHex-2-PyP (15 ± 4 versus 10 ± 5; $P = 0.002$; see Fig. 3). Cortical, subcortical, and total infarct volumes were decreased in rats treated with MnTnHex-2-PyP (Fig. 3).

**Experiment 4: 90-Min MCAO, Treatment Onset 6 h after Reperfusion Onset.** Physiologic values were similar to those obtained in the 5-min after MCAO onset treatment study and therefore are not reported. Rats treated with MnTnHex-2-PyP had decreased neurologic deficit ($P = 0.04$) (Fig. 4). Whereas cortical infarct size was substantially reduced by MnTnHex-2-PyP ($P = 0.01$), there was no effect in the subcortex ($P = 0.58$), which may be consistent with penumbral salvage at this late treatment interval. Total infarct size was decreased by 37% in rats treated with MnTnHex-2-PyP ($P = 0.03$) (Fig. 4). Representative histologic sections are provided in Fig. 5.

**Experiment 5: 90-Min MCAO, Treatment Onset 6 h after Reperfusion Onset/Validation with Laser Doppler Flowmetry.** Fifteen rats were randomly assigned to the MnTnHex-2-PyP group and 17 to vehicle (saline). No rats were excluded from analysis. Three MnTnHex-2-PyP and two vehicle-treated rats died during the recovery interval from unknown causes. Physiologic values were similar to those reported in Table 2. There were no statistically significant differences between groups. LDF values are depicted in

TABLE 1

Redox characteristics of MnPorphyrins (metal-centered reduction potential, $E_{1/2}$) (Batinic-Haberle et al., 2010a), their reactivity toward $O_2^{\cdot-}$ (as described by rate constant for the catalysis of $O_2^{\cdot-}$ dismutation, log $k_{cat}$) (Batinic-Haberle et al., 2010a), and $ONOO^-$ (as described by the rate of $ONOO^-$ reduction, log $k_{red}$) (Batinic-Haberle et al., 2010a), and mouse brain concentrations

Dose corrected values are normalized to 1 mg of drug per kg body weight. Reference values are given for native SOD $E_{1/2}$ (Vance and Miller, 1998) [log $k_{cat}(O_2^{\cdot-})$] (Goldstein et al., 2006) and the native $ONOO^-$ reductase (its role in vivo is presumed based on the high rate constant), peroxiredoxin [log $k_{red}$ ($ONOO^-$)] (Trujillo et al., 2007). The log $P_{OW}$ value is calculated using the equation log $P_{ow}$=0.96 × nC − 8.82, for MnTE-2-PyP, where nC is a number of carbon atoms in the alkyl chain. The experimentally determined value is provided for MnTnHex-2-PyP.

| Compound | $E_{1/2}$[a] | log $k_{cat}(O_2^{\cdot-})$ | log $k_{red}(ONOO^-)$ | log $P_{ow}$ | Brain | Dose Corrected Values |
|---|---|---|---|---|---|---|
| | | | | | *nM* | |
| Native Cu-Zn SOD | ~+300 | ~9.1 | 3.97[b] | | | |
| Native peroxiredoxin | | | 8.20 | | | |
| MnTE-2-PyP | +228 | 7.76 | 7.53 | −6.89 | 11[c] | 1.1 |
| MnTnHex-2-PyP | +314 | 7.48 | 7.11 | −2.76 | 19[d] | 9.5 |

[a] $E_{1/2}$ relates to Mn(III)P/Mn(II)P redox couple.
[b] Alvarez et al. (2004).
[c] MnTE-2-PyP mouse brain concentrations 24 h after a single 10 mg/kg i.p. injection (data previously reported in Spasojevic et al., 2008).
[d] MnTnHex-2-PyP mouse brain concentrations 24 h after a single 2 mg/kg i.p. injection (5-fold lower dose; see *Materials and Methods* and *Results*).

Fig. 6A. There was no difference between groups ($P$ = 0.67). Neurologic scores were improved by MnTnHex-2-PyP ($P$ = 0.002; Fig. 6B). As in experiment 4, MnTnHex-2-PyP decreased cortical (vehicle = 177 ± 33 versus MnTnHex-2-PyP = 140 ± 53 $mm^3$; $P$ = 0.04) and total infarct size ($P$ = 0.01; Fig. 6C). In contrast to experiment 4, there was also a decrease in subcortical infarct size (vehicle = 69 ± 16 versus MnTnHex-2-PyP = 51 ± 19 $mm^3$; $P$ = 0.02). Total infarct volume correlated with neurologic score ($P$ = 0.0004).

TABLE 2

Physiologic values for 90-min MCAO, treatment onset 5 min after reperfusion onset

All values are mean ± S.D.

| | Vehicle | MnTnHex-2-PyP |
|---|---|---|
| *n* | 17 | 18 |
| Preischemia body weight, g | 255 ± 14 | 262 ± 14 |
| Body weight 7 days after ischemia, g | 239 ± 51 | 275 ± 32* |
| Body weight change, g | −17 ± 47 | +14 ± 27* |
| 10 min preischemia, g | | |
| MAP, mm Hg | 81 ± 10 | 83 ± 7 |
| Arterial pH | 7.44 ± 0.04 | 7.43 ± 0.04 |
| $PaCO_2$, mm Hg | 38 ± 4 | 35 ± 3* |
| $PaO_2$, mm Hg | 163 ± 27 | 156 ± 23 |
| Blood glucose, mg/dl | 75 ± 11 | 72 ± 8 |
| Hematocrit, % | 42 ± 2 | 41 ± 2* |
| Pericranial temperature, °C | 37.5 ± 0.1 | 37.5 ± 0.1 |
| 45 min after ischemia onset | | |
| MAP, mm Hg | 76 ± 13 | 75 ± 10 |
| Arterial pH | 7.41 ± 0.05 | 7.41 ± 0.07 |
| $PaCO_2$, mm Hg | 39 ± 6 | 38 ± 5 |
| $PaO_2$, mm Hg | 167 ± 13 | 160 ± 17 |
| Pericranial temperature, °C | 37.5 ± 0.1 | 37.5 ± 0.1 |
| 10 min after ischemia | | |
| MAP, mm Hg | 73 ± 6 | 72 ± 7 |
| Arterial pH | 7.39 ± 0.06 | 7.38 ± 0.07 |
| $PaCO_2$, mm Hg | 40 ± 5 | 39 ± 6 |
| $PaO_2$, mm Hg | 173 ± 13 | 171 ± 15 |
| Pericranial temperature, °C | 37.5 ± 0.1 | 37.5 ± 0.1 |

* $P < 0.05$.

**Experiment 6: Brain TNF-α and IL-6.** Concentrations of cerebral proinflammatory cytokines, TNF-α and IL-6, were decreased at 24 h after MCAO in rats treated with MnTnHex-2-PyP (Fig. 7).

**Experiment 7: NF-κB Nuclear DNA Binding.** To determine whether the decrease in TNF-α and IL-6 proinflammatory cytokine synthesis was mediated by NF-κB signaling pathway inhibition as observed previously with MnTE-2-PyP in an in vitro system (Tse et al., 2004), electromobility-shift assays were performed with nuclear extracts obtained from 90-min MCAO rats treated with MnTnHex-2-PyP or vehicle (Fig. 8). Rats treated with vehicle exhibited an increase in NF-κB activation. Treatment with MnTnHex-2-PyP inhibited nuclear NF-κB binding that corresponded to a decrease in nuclear translocation of NF-κB as indicated by NF-κB p65 supershift analysis.

**Experiment 8: SAH Outcome.** No mice were excluded from analysis. Three mice in the vehicle group and one mouse in the MnTnHex-2-PyP group died during the 72-h recovery interval. Among survivors, treatment with MnTnHex-2-PyP improved neurologic score at 3 days after SAH ($P$ = 0.02; Fig. 8). There was no difference between groups for hemorrhage grade (vehicle = 3 ± 1; MnTnHex-2-PyP = 3 ± 0; $P$ = 0.53). MnTnHex-2-PyP increased diameters of the internal carotid,

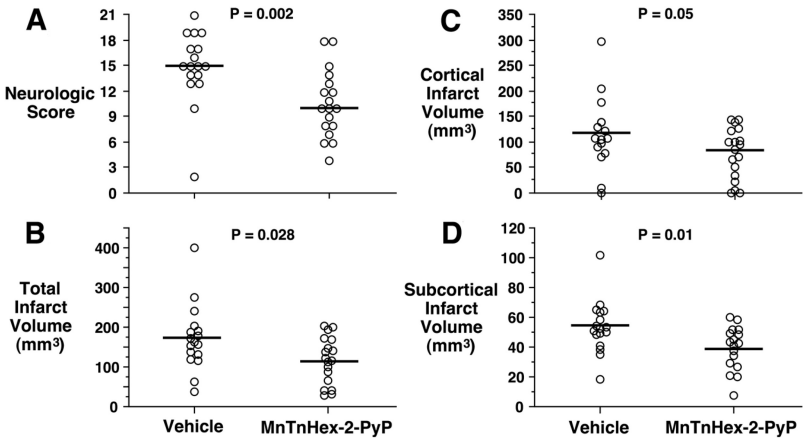


**Fig. 3.** Rats were subjected to 90 min of MCAO. Five minutes after reperfusion onset, intravenous treatment was begun with vehicle or 225 μg/kg MnTnHex-2-PyP. MnTnHex-2-PyP (225 μg/kg) was given subcutaneously twice daily for 7 days after which neurologic function was assessed. Circles indicate individual animal values. A, neurologic scores at 7 days after MCAO. Horizontal lines indicate group median values. 0 = no neurologic deficit. B to D, total cerebral, cortical, and subcortical infarct volumes measured 7 days after MCAO, respectively. Horizontal lines indicate group mean values.

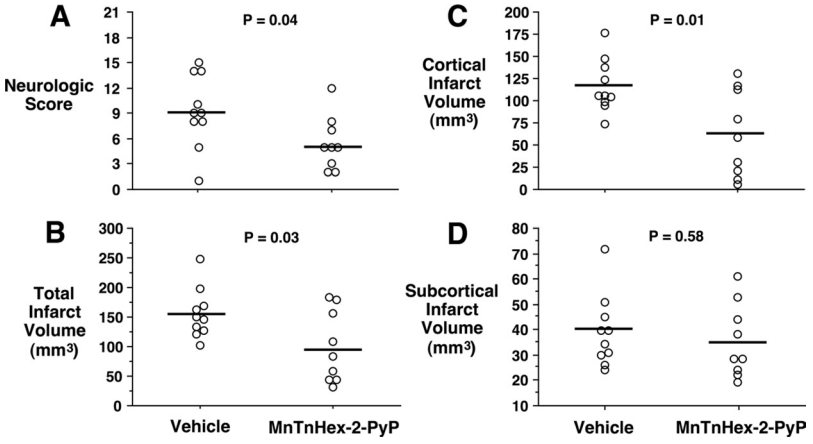


**Fig. 4.** Rats were subjected to 90 min of MCAO. Six hours after reperfusion onset, they were treated with intra-arterial vehicle or 225 μg/kg MnTnHex-2-PyP. MnTnHex-2-PyP (225 μg/kg) was given subcutaneously twice daily for 7 days after which neurologic function was assessed. Circles indicate individual animal values. A, neurologic scores at 7 days after MCAO. Horizontal lines indicate group median values. 0 = no neurologic deficit. B to D, total cerebral, cortical, and subcortical infarct volumes, respectively, measured 7 days after MCAO. Horizontal lines indicate group mean values.

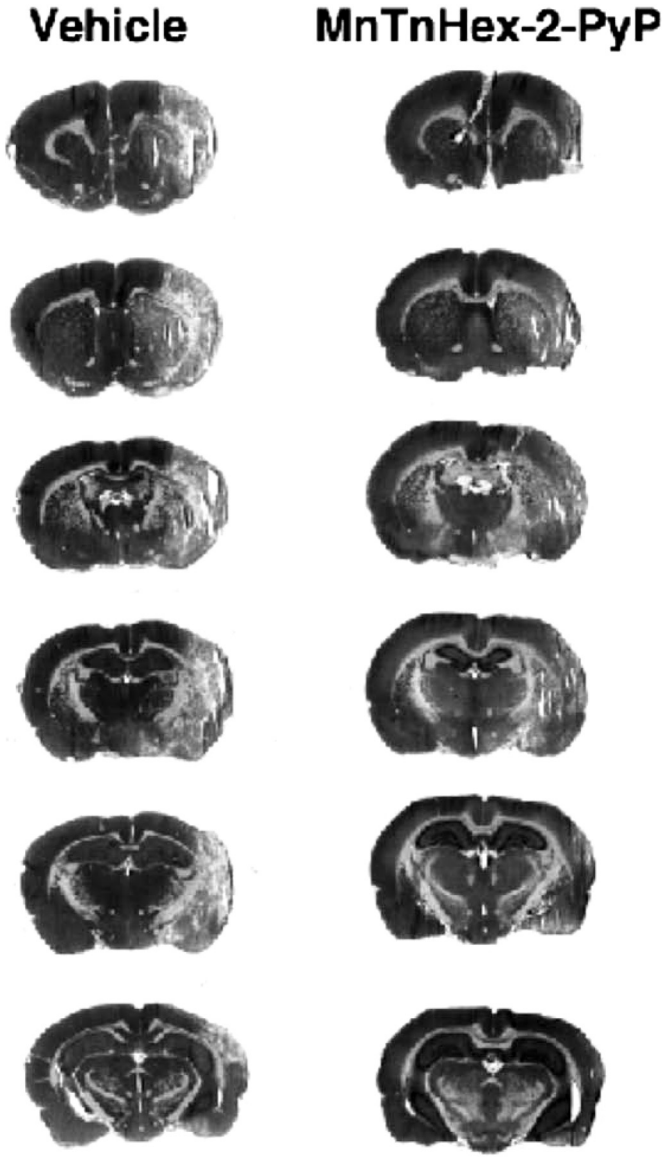


**Fig. 5.** Serial hematoxylin and eosin-stained coronal sections from rats subjected to 90 min of MCAO with treatment beginning 6 h after reperfusion onset and continuing for 7-day recovery. Vehicle (left) and MnTnHex-2-PyP (right) representative sections were chosen from the rat in each treatment group having total infarct volume most similar to the respective group mean values.

middle, and anterior cerebral arteries ipsilateral to the ACA perforation (Figs. 9 and 10). There was no difference between groups in basilar artery diameter (vehicle = 198 ± 19; MnTnHex-2-PyP = 200 ± 17; $P = 0.73$; sham = 193 ± 5) indicating similar perfusion conditions between groups during vessel casting. There was no effect of MnTnHex-2-PyP on MAP ($P = 0.09$; 5 min preinjection = 81 ± 4 mm Hg; 60 min after injection = 80 ± 4 mm Hg).

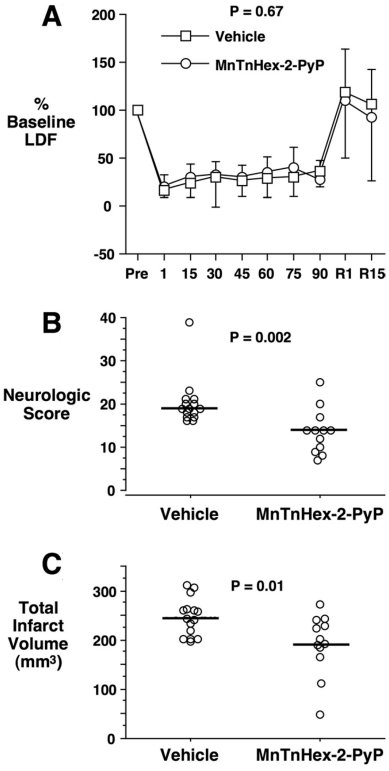


**Fig. 6.** Rats were subjected to 90 min of MCAO with continuous LDF monitoring. Six hours after reperfusion onset, they were treated with intra-arterial vehicle or 225 μg/kg MnTnHex-2-PyP. MnTnHex-2-PyP (225 μg/kg) was given subcutaneously twice daily for 7 days after which neurologic function was assessed. A, mean ± S.D. LDF values for the two groups. Values were converted to percentage baseline values measured 15 min before MCAO onset. R1 and R15 represent values taken at 1 and 15 min after reperfusion onset, respectively. B, neurologic scores at 7 days after MCAO. Circles indicate individual animal values. Horizontal lines indicate group median values. 0 = no neurologic deficit. C, total cerebral infarct volumes measured 7 days after MCAO. Circles indicate individual animal values. Horizontal lines indicate group mean values.

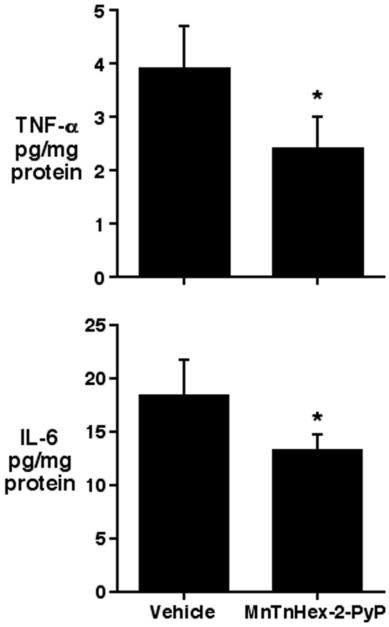


**Fig. 7.** Rats were subjected to 90 min of MCAO. Five minutes after onset of reperfusion, rats were randomly treated with vehicle ($n = 3$) or 225 μg/kg i.v. MnTnHex-2-PyP ($n = 3$) followed by subcutaneous vehicle or 225 μg/kg MnTnHex-2-PyP, respectively, at 12 and 18 h after MCAO. Brains were harvested at 24 h after MCAO, and TNF-α and IL-6 protein concentrations were analyzed by rat-specific enzyme-linked immunosorbent assay. Values represent mean ± S.D. Both TNF-α and IL-6 concentrations were decreased by MnTnHex-2-PyP. *, $P < 0.05$.

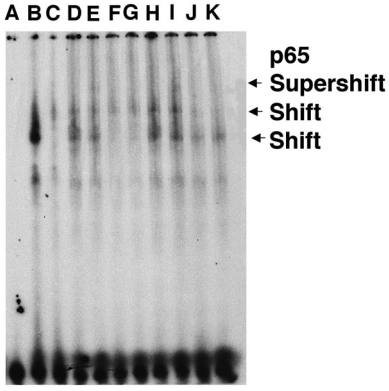


**Fig. 8.** Intravenous MnTnHex-2-PyP (hexyl) decreased after ischemic NF-κB DNA binding to a κB consensus oligo. Data are from four rats subjected to 90 min of MCAO and then treated with vehicle or hexyl (225 μg/kg i.v.). Six hours later, ischemic brain was harvested to obtain nuclear extracts (2.5 μg). Lanes A to C, control [A, probe only; B, positive control (HeLa nuclear extract); C, unlabeled competitor]. Lanes D and E, rat 1 (vehicle) without (D) and with (E) p65 antibody. Lanes F and G, rat 2 (hexyl) without (F) and with (G) p65 antibody. Lanes H and I, vehicle rat 3 with (H) and (I) without p65. Lanes J and K, rat 4 (hexyl) with (J) and without (K) p65. Two slower migrating DNA binding complexes were observed (shift). The proteins in the slower migrating complexes were identified by supershift analysis with 1 μg of p65-specific antibody. Marked reduction in NF-κB binding is seen in rats 2 and 4 (lanes F, G, J, and K; both hexyl).

## Discussion

Hexyl substitution in the *ortho* positions of four *meso* pyridyl groups in MnPorphyrin, so as to create MnTnHex-2-PyP, increases lipophilicity by more than four orders of magnitude relative to the ethyl analog MnTE-2-PyP (Batinić-Haberle et al., 2011b). This allowed parenteral MnTnHex-2-PyP treatment in rats subjected to transient MCAO, resulting in a substantive decrease in cerebral infarct size and neurologic deficit, even when treatment began 6 h after reperfusion onset. Efficacy of delayed onset treatment was reproducible in separate experiments. MnTnHex-2-PyP attenuated NF-κB DNA binding and NF-κB regulated cytokine expression. In mice subjected to SAH, parenteral MnTnHex-2-PyP decreased cerebral vessel narrowing and neurologic deficits, indicating efficacy in more than one form of acute CNS injury.

A major obstacle to MnPorphyrin development for CNS therapeutic applications has been its limited bioavailability. The cationic charges on pyridyls, essential to the high SOD-like activity of MnPorphyrins (i.e., a net 5+ molecular charge), contribute to low lipophilicity. Although MnTE-2-PyP crosses the BBB (Sheng et al., 2002b; Spasojevic et al., 2008a), the mouse brain concentration within 24 h after intraperitoneal injection is markedly greater with MnTnHex-2-PyP than MnTE-2-PyP (Table 1). This should have an impact on the onset of therapeutic action and efficacy. Based on mouse pharmacokinetic analysis with 2 mg/kg i.p. MnTnHex-2-PyP, the normalized brain concentration is 9.5 nM, whereas it is 1.1 nM (wet weight) for MnTE-2-PyP given by the same intraperitoneal route (Spasojevic et al., 2008a). Therefore, increasing lipophilicity by a factor of 13,500 by hexyl substitution allows an accumulation ~9-fold greater than the hydrophilic MnTE-2-PyP (Table 1). Consequently, MnTnHex-2-PyP doses required to obtain efficacy were markedly less than doses required for MnTE-2-PyP (Mackensen et al., 2001; Sheng et al., 2002b). Similar MnTnHex-2-PyP doses have been found effective in other in vivo injury models (Batinić-Haberle et al., 2010b). For example, a single 50 μg/kg i.v. MnTnHex-2-PyP dose protects against renal dysfunction after ischemia/reperfusion (Saba et al., 2007). Furthermore, 100 μg/kg i.p. MnTnHex-2-PyP given daily for 6 weeks was efficacious in the study of rat ocular hypertension (Dogan et al., 2011). Further investigation is necessary to determine a full pharmacokinetic spectrum for MnTnHex-2-PyP in both normal and ischemic brain. It is likely that pharmacokinetics in injured tissue will be different in the presence of BBB disruption (Sheng et al., 2002b).

Lipophilicity also plays a role in subcellular distribution of MnPorphyrins. Prior work demonstrated compartmentalization of MnTE-2-PyP in mitochondria (Spasojevic et al., 2007), which would seem favorable to ameliorating oxidative stress. Independent studies on *Saccharomyces cerevisiae* yeast and mouse heart showed that mitochondrial accumulation is related to alkyl chain length (Spasojevic et al., 2010). Lipophilicity increases 10-fold for each $CH_2$ group added. Thus, the hexyl analog is 13,500-fold more lipophilic than MnTE-2-PyP (Kos et al., 2009; Pollard et al., 2009; Batinić-Haberle et al., 2010a). Increased lipophilicity and resultant mitochondrial accumulation probably contributes to the higher efficacy of MnTnHex-2-PyP relative to MnTE-2-PyP (Batinić-Haberle et al., 2009b, 2011b; Kos et al., 2009; Spasojevic et al., 2010, 2011).

MnPorphyrins are also likely to accumulate in the nucleus, driven by negatively charged phosphates of nucleic acids. Like SOD during catalysis of superoxide dismutation, MnPorphyrins can accept and donate electrons at similar rates, which allow some analogs to be almost as potent as SOD (Batinić-Haberle et al., 2004). They also have the potential to act as oxidizing agents in certain environments.

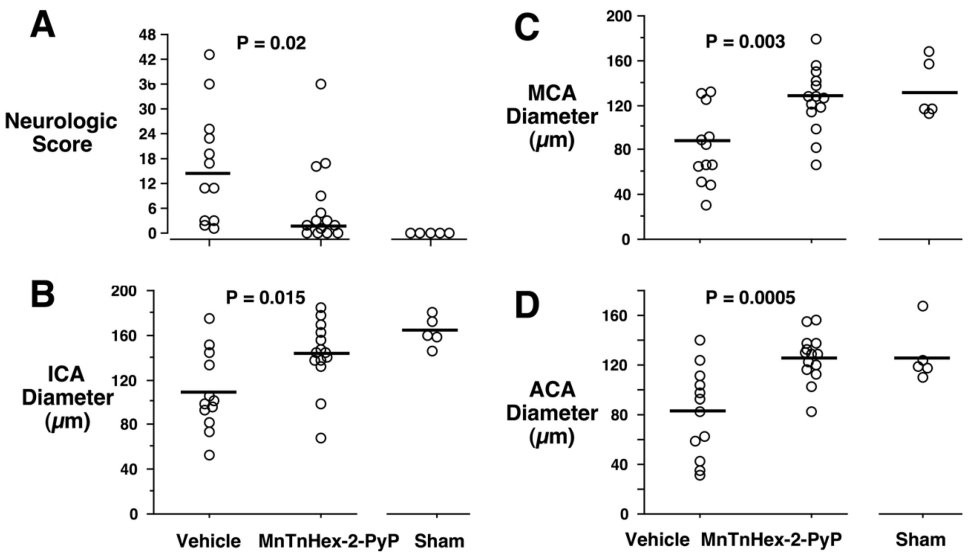


**Fig. 9.** Mice underwent filament perforation of the right anterior cerebral artery resulting in subarachnoid hemorrhage. Mice received intraperitoneal vehicle or MnTnHex-2-PyP over a 72-h recovery period. A, neurologic function was then assessed. Circles indicate individual animal values. Horizontal lines indicate group median values. 0 = no neurologic deficit. B to D, mice then underwent in situ vascular casting and measurement of diameters of the ipsilateral ICA (B), MCA (C), and ACA (D). Sham-operated mice provide normal reference values. Circles indicate individual animal values. Horizontal bars indicate group mean values.

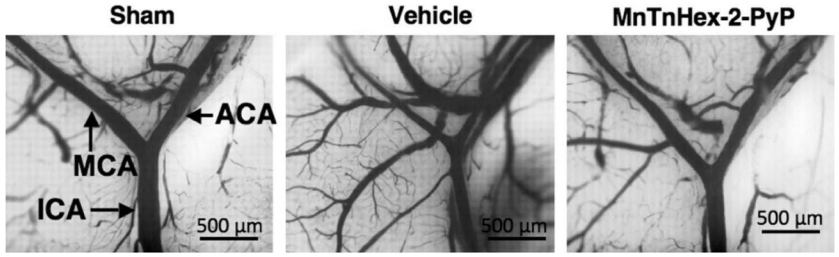


**Fig. 10.** Intravascular casted ICA bifurcating into the MCA and ACA. Decreased intraluminal diameters are seen in vehicle-treated mice subjected to subarachnoid hemorrhage. Vessel narrowing was decreased in mice treated with MnTnHex-2-PyP.

This may explain their pro-oxidative action in the nucleus (Batinić-Haberle et al., 2010b). Tse et al. (2004), using an in vitro system, reported that MnTDE-2-ImP oxidizes cysteine 62 residue of p50, thereby inhibiting DNA binding to its canonical κB motifs. The same has been found in an in vitro system for MnTnHex-2-PyP (Batinić-Haberle et al., 2010b). Our study has now shown inhibition of in vivo NF-κB-DNA binding by MnTnHex-2-PyP, consistent with previous observations for intracerebroventricular MnTDE-2-ImP (Sheng et al., 2009). Furthermore, in the presence of $H_2O_2$, Mn-TE-2-PyP glutathionylates p65 of NF-κB, thereby depleting glutathione and inhibiting NF-κB DNA binding (Jaramillo et al., 2010). MnPorphyrins prevent activation of other transcription factors including hypoxia-inducible factor 1α, activator protein-1, and Sp1 (Batinić-Haberle et al., 2010b). These properties would be expected to result in delayed effects on tissue subjected to oxidative stress. Data regarding NF-κB inhibition in MCAO support the proposal that delayed MnPorphyrin therapy targets genomic responses to reperfusion, resulting in altered inflammatory and plausibly apoptotic sequels to the ischemic insult. The study of MnPorphyrin therapy should be expanded to other redox-regulated transcription factors and response gene expression in the context of acute CNS injury.

Rats are known to exhibit a species-specific arterial hypotensive response to MnPorphyrins (Ross et al., 2002). The mechanism for this remains undefined, and this also has limited preclinical MnPorphyrin evaluation as potential clinical therapeutics. Although short-term recovery in the mouse is routine, few laboratories are able to sustain postischemic survival in this species beyond 24 to 72 h. Longer recovery intervals are necessary to define potential clinical relevance. To obviate the likely confound associated with arterial hypotension and cerebral perfusion pressure in the context of focal ischemia and reperfusion, we have previously studied MnPorphyrins administered as intracerebroventricular injections in rats, which enabled outcome analyses as late as 8 weeks after MCAO (Sheng et al., 2009). It was learned that single bolus MnPorphyrin treatment did not provide sustained protection beyond an observation interval of 1 week. In contrast, continuous intracerebroventricular infusion for 1 week after MCAO provided persistent decrease in cerebral infarct size and neurologic deficit at 8 weeks after MCAO. For that reason, we elected to sustain parenteral MnTnHex-2-PyP for the full 7-day recovery interval in the current investigation. Subcutaneous injection was selected to avoid chronic venous cannulation or osmotic pump implantation, which could confound functional analysis. This treatment paradigm was well tolerated with respect to postischemic body weight (Table 2), suggesting lack of acute major organ toxicity. Supporting this, the current pharmacokinetic study performed over a 7-day interval showed no change in body weight or rotarod performance in normal rats given two doses per day of 225 μg/kg i.p. MnTnHex-2-Pyp, despite accumulating concentrations in brain and plasma (Fig. 2). We attribute this to the markedly smaller MnTnHex-2-PyP dose required to achieve efficacy, which obviated arterial hypotension as a potential confound in the rat (see *Dose Finding Studies*) and now allows use of this species for further preclinical analysis. Additional work is required to confirm that parenteral MnTnHex-2-PyP will provide sustained protection against focal ischemia at longer outcome intervals, including dose-response analysis. More work is also required to define the minimum duration of treatment necessary to

obtain maximal improvement in long-term outcome, as well as dosing regimens necessary to rapidly achieve and sustain therapeutic brain concentrations.

It is noteworthy that MnPorphyrins have previously been shown to have no effect on postischemic body temperature (Mackensen et al., 2001; Sheng et al., 2002b). Pericranial temperature was controlled and maintained normothermic in all animals during MCAO. These data make it unlikely that the improved outcomes observed in these experiments could be attributed to a nonspecific effect on systemic physiology.

A different MnPorphyrin side-chain substitution (AEOL11207) has been tested using orogastric administration with encouraging results in a Parkinson's disease model (Liang et al., 2007). Increased lipophilicity was obtained by eliminating the 4+ positive charge of the parent molecule. However, this also eliminated electrostatic facilitation of negatively charged superoxide to approach manganese for reduction. Such facilitation accounts for more than two orders of magnitude decrease in SOD-like efficacy when the compound that carries no charges is compared with the MnPorphyrin that carries four positive charges on the periphery (Batinić-Haberle et al., 2010a). In contrast, MnTnHex-2-PyP retains SOD activity in the face of improved lipophilicity. Lipophilicity and SOD activity both are critical in defining efficacy (Batinić-Haberle et al., 2009b; Kos et al., 2009). Despite similar SOD activity, MnPorphyrins with decreased lipophilicity must be given in larger doses to obtain a similar CNS effect. For example, an intraperitoneal MnTE-2-PyP dose 30-fold greater than MnTnHex-2-PyP is required to inhibit morphine antinociceptive tolerance in mice, despite both molecules having similar SOD activity (Batinić-Haberle et al., 2009b; Kos et al., 2009). The relative balance between net positive charge and lipophilicity is likely critical to optimize bioavailability and thus local efficacy.

SAH is also associated with oxidative stress culminating in arterial narrowing and ischemic injury to brain. We used an established mouse SAH model (Parra et al., 2002), previously used to first demonstrate efficacy of HMG-CoA reductase inhibitors in ameliorating this disorder (McGirt et al., 2002). In the case of MnTnHex-2-PyP, substantial benefit was again observed. There has been one prior attempt to treat experimental SAH with an anionic MnPorphyrin, MnTBAP (Aladag et al., 2003). MnTBAP attenuated narrowing of the rat basilar artery measured 5 days after intracisternal double injection of autologous blood. Although encouraging, this work required confirmation, because neurologic function was not assessed, and commercial MnTBAP preparations have insufficient purity to allow conclusions specific to MnPorphyrin chemistry (Reboucas et al., 2008). The current experiment showed major beneficial effect of parenteral MnTnHex-2-PyP on both vessel narrowing and neurologic function after SAH, thereby confirming earlier work, but with a more completely characterized molecule. For example, SAH caused a mean 38% decrease in MCA diameter relative to sham-operated mice. Treatment with MnTnHex-2-PyP maintained mean MCA diameter within 8% of sham values despite an identical hemorrhage grade. Mechanisms of efficacy of MnTnHex-2-PyP in SAH will be the subject of further investigation. Evidence from the MCAO model reported above suggests that MnTnHex-2-PyP effects on NF-κB activation and inflammatory gene expression may be involved in this mechanism of vasospasm progression (Zhou et al., 2007), but this remains to be tested. It is noteworthy that although not performed concurrently but examined in an identical SAH model, the effect size of MnTnHex-2-PyP exceeded that of simvastatin when treatment was begun postictus (e.g., after SAH MCA diameter increased by 24% with simvastatin versus 48% with MnTnHex-2-PyP) (McGirt et al., 2002). Because simvastatin is clinically available and remains of interest for the treatment of clinical SAH (Kramer and Fletcher, 2010), direct comparison of these two pharmacologic interventions is warranted.

In summary, we have evaluated a lipophilic MnPorphyrin that retains major redox activity, but allows rapid and substantive BBB penetration when given parenterally. The major impediment to development of MnPorphyrins for CNS indications has been hydrophilicity that prevented appropriate preclinical testing and demonstration of efficacy sufficient to warrant clinical investigation for acute CNS injury disorders. Here, we demonstrated that parenteral treatment with the lipophilic MnTnHex-2-PyP decreased focal transient ischemic brain injury with treatment onset beginning as late as 6 h after onset of reperfusion from temporary MCAO, attenuated NF-κB activation, and down-regulated IL-6 and TNF-α expression. These effects are consistent with the efficacy reported for other MnPorphyrins that required intracerebroventricular administration (Mackensen et al., 2001; Sheng et al., 2002b, 2009). Parenteral MnTnHex-2-PyP also significantly attenuated delayed arterial vasoconstriction and neurologic deficits associated with SAH. Thus, synthesis of lipophilic MnPorphyrins might constitute a breakthrough for their use as therapeutics in acute brain injury. Direct experimental comparison/use with current therapy (e.g., nimodipine for SAH and tissue plasminogen activator for thrombolysis in ischemic stroke), as well as efficacy in nonreperfusion states (e.g., permanent MCAO) will be important to define before clinical evaluation of such compounds.

#### Authorship Contributions

*Participated in research design:* Sheng, Tse, Piganelli, Batinic-Haberle, and Warner.

*Conducted experiments:* Sheng, Spasojevic, Tse, Jung, Hong, Zhang, and Warner.

*Contributed new reagents or analytic tools:* Spasojevic and Batinic-Haberle.

*Performed data analysis:* Sheng, Spasojevic, and Warner.

*Wrote or contributed to the writing of the manuscript:* Sheng, Tse, Piganelli, Batinic-Haberle, and Warner.

#### References

Aladag MA, Turkoz Y, Sahna E, Parlakpinar H, and Gul M (2003) The attenuation of vasospasm by using a sod mimetic after experimental subarachnoidal haemorrhage in rats. *Acta Neurochir (Wien)* **145:**673–677.

Alvarez B, Demicheli V, Durán R, Trujillo M, Cerveñansky C, Freeman BA, and Radi R (2004) Inactivation of human Cu,Zn superoxide dismutase by peroxynitrite and formation of histidinyl radical. *Free Radic Biol Med* **37:**813–822.

Batinić-Haberle I, Benov L, Spasojević I, and Fridovich I (1998) The *ortho* effect makes manganese(III) *meso*-tetrakis (*N*-methylpyridinium-2-yl)porphyrin ($MnTM\text{-}2\text{-}PyP^{5+}$) a powerful and potentially useful superoxide dismutase mimic. *J Biol Chem* **273:**24521–24528.

Batinić-Haberle I, Cuzzocrea S, Rebouças JS, Ferrer-Sueta G, Mazzon E, Di Paola R, Radi R, Spasojević I, Benov L, and Salvemini D (2009a) Pure MnTBAP selectively scavenges peroxynitrite over superoxide: comparison of pure and commercial MnTBAP samples to MnTE-2-PyP in two models of oxidative stress injury, an SOD-specific *Escherichia coli* model and carrageenan-induced pleurisy. *Free Radic Biol Med* **46:**192–201.

Batinić-Haberle I, Ndengele MM, Cuzzocrea S, Rebouças JS, Spasojević I, and Salvemini D (2009b) Lipophilicity is a critical parameter that dominates the efficacy of metalloporphyrins in blocking the development of morphine antinoci-

ceptive tolerance through peroxynitrite-mediated pathways. *Free Radic Biol Med* **46:**212–219.

Batinić-Haberle I, Rajic Z, Tovmasyan A, Reboucas JS, Ye X, Leong KW, Dewhirst MW, Vujaskovic Z, Benov L, and Spasojevic I (2011a) Diverse functions of cationic Mn(III) substituted *N*-pyridylporphyrins, known as SOD mimics. *Free Radic Biol Med* doi:10.1016/j.freeradbiomed.2011.04.046.

Batinić-Haberle I, Reboucas JS, Benov L, and Spasojevic I (2011b) Chemistry, biology and medical effects of water soluble metallopophyrins, in *Handbook of Porphyrin Science* (Kadish KM, Smith K, Guillard R eds) pp 291–393, World Scientific, Singapore.

Batinić-Haberle I, Rebouças JS, and Spasojević I (2010a) Superoxide dismutase mimics: chemistry, pharmacology, and therapeutic potential. *Antioxid Redox Signal* **13:**877–918.

Batinic-Haberle I, Spasojevic I, Stevens RD, Hambright P, and Fridovich I (2002) Manganese(III) meso-tetrakis(ortho-*N*-alkylpyridyl)porphyrins. Synthesis, characterization, and catalysis of $O_2^{\cdot-}$ dismutation. *J Chem Soc Dalton Trans* 2689–2696.

Batinic-Haberle I, Spasojevic I, Stevens RD, Hambright P, Neta P, Okado-Matsumoto A, and Fridovich I (2004) New class of potent catalysts of $O_2^{\cdot-}$ dismutation. Mn(III) ortho-methoxyethylpyridyl- and di-ortho-methoxyethylimidazolylporphyrins. *Dalton Trans* 1696–1702.

Batinic-Haberle I, Spasojevic I, Tse HM, Tovmasyan A, Rajic Z, St Clair DK, Vujaskovic Z, Dewhirst MW and Piganelli JD (2010b) Design of Mn porphyrins for treating oxidative stress injuries and their redox-based regulation of cellular transcriptional activities. *Amino Acids* doi:10.1007/s00726-010-0603-6.

DeFreitas-Silva G, Rebouças JS, Spasojević I, Benov L, Idemori YM, and Batinić-Haberle I (2008) SOD-like activity of Mn(II) β-octabromo-meso-tetrakis(*N*-methylpyridinium-3-yl)porphyrin equals that of the enzyme itself. *Arch Biochem Biophys* **477:**105–112.

Dogan S, Unal M, Ozturk N, Yargicoglu P, Spasojevic I, Batinc-Haberle I, and Aslan M (2011) Manganese porphyrin reduces retinal injury induced by ocular hypertension. *Exp Eye Res* doi:10.1016/j.exer.2011.05.008.

Goldstein S, Fridovich I, and Czapski G (2006) Kinetic properties of Cu,Zn-superoxide dismutase as a function of metal content–order restored. *Free Radic Biol Med* **41:**937–941.

Hall ED, Pazara KE, Braughler JM, Linseman KL, and Jacobsen EJ (1990) Non-steroidal lazaroid U78517F in models of focal and global ischemia. *Stroke* **21:** III83–III87.

Jaramillo MD, Briejl MM, and Tome ME (2010) Manganese porphyrin glutathionylates the p65 subunit of NF-κB to potentiate glucocorticoid-induced apoptosis in lymphoma. *Free Radic Biol Med* **49:**S63.

Kamii H, Kato I, Kinouchi H, Chan PH, Epstein CJ, Akabane A, Okamoto H, and Yoshimoto T (1999) Amelioration of vasospasm after subarachnoid hemorrhage in transgenic mice overexpressing CuZn-superoxide dismutase. *Stroke* **30:**867–871; discussion 872.

Kos I, Rebouças JS, DeFreitas-Silva G, Salvemini D, Vujaskovic Z, Dewhirst MW, Spasojević I, and Batinić-Haberle I (2009) Lipophilicity of potent porphyrin-based antioxidants: comparison of ortho and meta isomers of Mn(III) *N*- alkylpyridylporphyrins. *Free Radic Biol Med* **47:**72–78.

Kramer AH and Fletcher JJ (2010) Statins in the management of patients with aneurysmal subarachnoid hemorrhage: a systematic review and meta-analysis. *Neurocrit Care* **12:**285–296.

Liang LP, Huang J, Fulton R, Day BJ, and Patel M (2007) An orally active catalytic metalloporphyrin protects against 1-methyl-4-phenyl-1,2,3,6-tetrahydropyridine neurotoxicity in vivo. *J Neurosci* **27:**4326–4333.

Longa EZ, Weinstein PR, Carlson S, and Cummins R (1989) Reversible middle cerebral artery occlusion without craniectomy in rats. *Stroke* **20:**84–91.

Mackensen GB, Patel M, Sheng H, Calvi CL, Batinic-Haberle I, Day BJ, Liang LP, Fridovich I, Crapo JD, Pearlstein RD, et al. (2001) Neuroprotection from delayed postischemic administration of a metalloporphyrin catalytic antioxidant. *J Neurosci* **21:**4582–4592.

Marshall JW, Duffin KJ, Green AR, and Ridley RM (2003) NXY-059, a free radical-trapping agent, substantially lessens the functional disability resulting from cerebral ischemia in a primate species. *Stroke* **32:**190–198.

McGirt MJ, Lynch JR, Parra A, Sheng H, Pearlstein RD, Laskowitz DT, Pelligrino DA, and Warner DS (2002) Simvastatin increases endothelial nitric oxide synthase and ameliorates cerebral vasospasm resulting from subarachnoid hemorrhage. *Stroke* **33:**2950–2956.

Niizuma K, Endo H, and Chan PH (2009) Oxidative stress and mitochondrial dysfunction as determinants of ischemic neuronal death and survival. *J Neurochem* **109(Suppl 1):**133–138.

Parra A, McGirt MJ, Sheng H, Laskowitz DT, Pearlstein RD, and Warner DS (2002) Mouse model of subarachnoid hemorrhage associated cerebral vasospasm: methodological analysis. *Neurol Res* **24:**510–516.

Pollard JM, Reboucas JS, Durazo A, Kos I, Fike F, Panni M, Gralla EB, Valentine JS, Batinic-Haberle I, and Gatti RA (2009) Radioprotective effects of manganese-containing superoxide dismutase mimics on ataxia-telangiectasia cells. *Free Radic Biol Med* **47:**250–260.

Rebouças JS, Spasojević I, and Batinić-Haberle I (2008) Quality of potent Mn porphyrin-based SOD mimics and peroxynitrite scavengers for pre-clinical mechanistic/therapeutic purposes. *J Pharm Biomed Anal* **48:**1046–1049.

Ross AD, Sheng H, Warner DS, Piantadosi CA, Batinic-Haberle I, Day BJ, and Crapo JD (2002) Hemodynamic effects of metalloporphyrin catalytic antioxidants: structure-activity relationships and species specificity. *Free Radic Biol Med* **33:**1657–1669.

Saba H, Batinic-Haberle I, Munusamy S, Mitchell T, Lichti C, Megyesi J, and MacMillan-Crow LA (2007) Manganese porphyrin reduces renal injury and mitochondrial damage during ischemia/reperfusion. *Free Radic Biol Med* **42:**1571–1578.

Sakai H, Sheng H, Yates RB, Ishida K, Pearlstein RD, and Warner DS (2007) Isoflurane provides long-term protection against focal cerebral ischemia in the rat. *Anesthesiology* **106:**92–99; discussion 98–110.

Sheng H, Batinc-Haberle I, and Warner DS (2002a) Catalytic antioxidants as novel pharmacologic approaches to treatment of ischemic brain injury. *Drug News Perspect* **15:**654–665.

Sheng H, Enghild JJ, Bowler R, Patel M, Batinić-Haberle I, Calvi CL, Day BJ, Pearlstein RD, Crapo JD, and Warner DS (2002b) Effects of metalloporphyrin catalytic antioxidants in experimental brain ischemia. *Free Radic Biol Med* **33:** 947–961.

Sheng H, Reynolds JD, Auten RL, Demchenko IT, Piantadosi CA, Stamler JS, and Warner DS (2011) Pharmacologically augmented S-nitrosylated hemoglobin improves recovery from murine subarachnoid hemorrhage. *Stroke* **42:**471–476.

Sheng H, Yang W, Fukuda S, Tse HM, Paschen W, Johnson K, Batinic-Haberle I, Crapo JD, Pearlstein RD, Piganelli J, et al. (2009) Long-term neuroprotection from a potent redox-modulating metalloporphyrin in the rat. *Free Radic Biol Med* **47:**917–923.

Shuaib A, Lees KR, Lyden P, Grotta J, Davalos A, Davis SM, Diener HC, Ashwood T, Wasiewski WW, Emeribe U, et al. (2007) NXY-059 for the treatment of acute ischemic stroke. *N Engl J Med* **357:**562–571.

Spasojevic I, Batinic-Haberle I, and Fridovich I (2000) Nitrosylation of manganese(II) tetrakis(*N*-ethylpyridinium-2-yl)porphyrin: a simple and sensitive spectrophotometric assay for nitric oxide. *Nitric Oxide* **4:**526–533.

Spasojević I, Chen Y, Noel TJ, Fan P, Zhang L, Rebouças JS, St Clair DK, and Batinić-Haberle I (2008a) Pharmacokinetics of the potent redox-modulating manganese porphyrin, MnTE-2-PyP(5+), in plasma and major organs of B6C3F1 mice. *Free Radic Biol Med* **45:**943–949.

Spasojević I, Chen Y, Noel TJ, Yu Y, Cole MP, Zhang L, Zhao Y, St Clair DK, and Batinić-Haberle I (2007) Mn porphyrin-based superoxide dismutase (SOD) mimic, MnIIITE-2-PyP5+, targets mouse heart mitochondria. *Free Radic Biol Med* **42:** 1193–1200.

Spasojevic I, Kos I, Benov LT, Rajic Z, Fels D, Dedeugd C, Ye X, Vujaskovic Z, Reboucas JS, Leong KW, et al. (2011) Bioavailability of metalloporphyrin-based SOD mimics is greatly influenced by a single charge residing on a Mn site. *Free Radic Res* **45:**188–200.

Spasojevic I, Sheng H, Warner DS, and Batinic-Haberle I (2008b) Metalloporphyrins are versatile and powerful therapeutics: biometrics of SOD, peroxyredoxin, and P450, at the *Second World Conference on Magic Bullets (Ehrlich II)*; 2008 Oct 3–5; Nurnberg, Germany.

Spasojevic I, Tovmasyan A, Rajic Z, Salvemini D, St. Clair D, Valentine JS, Vujaskovic Z, Gralla EB and Batinic-Haberle I (2010) Accumulation of porphyrin-based SOD mimics in mitochondria is proportional to their lipophilicity. *S. cerevisiae* study of ortho Mn(III) *N*- alkylpyridylporphyrins. *Free Radic Biol Med* **49:**S199.

Swanson RA, Morton MT, Tsao-Wu G, Savalos RA, Davidson C, and Sharp FR (1990) A semiautomated method for measuring brain infarct volume. *J Cereb Blood Flow Metab* **10:**290–293.

The RANTTAS Investigators (1996) A randomized trial of tirilazad mesylate in patients with acute stroke (RANTTAS). *Stroke* **27:**1453–1458.

Trujillo M, Clippe A, Manta B, Ferrer-Sueta G, Smeets A, Declercq JP, Knoops B, and Radi R (2007) Pre-steady state kinetic characterization of human peroxiredoxin 5: taking advantage of Trp84 fluorescence increase upon oxidation. *Arch Biochem Biophys* **467:**95–106.

Tse HM, Milton MJ, and Piganelli JD (2004) Mechanistic analysis of the immunomodulatory effects of a catalytic antioxidant on antigen-presenting cells: implication for their use in targeting oxidation-reduction reactions in innate immunity. *Free Radic Biol Med* **36:**233–247.

Vance CK and Miller AF (1998) A simple proposal that can explain the inactivity of metal-substituted superoxide dismutases. *J Am Chem Soc* **120:**461–467.

Warner DS, Ludwig PS, Pearlstein R, and Brinkhous AD (1995) Halothane reduces focal ischemic injury in the rat when brain temperature is controlled. *Anesthesiology* **82:**1237–1245; discussion 27A.

Warner DS, Sheng H, and Batinić-Haberle I (2004) Oxidants, antioxidants and the ischemic brain. *J Exp Biol* **207:**3221–3231.

Yokoo N, Sheng H, Mixco J, Homi HM, Pearlstein RD, and Warner DS (2004) Intraischemic nitrous oxide alters neither neurologic nor histologic outcome: a comparison with dizocilpine. *Anesth Analg* **99:**896–903, table of contents.

Zhang H, Joseph J, Gurney M, Becker D, and Kalyanaraman B (2002) Bicarbonate enhances peroxidase activity of Cu,Zn-superoxide dismutase. Role of carbonate anion radical and scavenging of carbonate anion radical by metalloporphyrin antioxidant enzyme mimetics. *J Biol Chem* **277:**1013–1020.

Zhou ML, Shi JX, Hang CH, Cheng HL, Qi XP, Mao L, Chen KF, and Yin HX (2007) Potential contribution of nuclear factor-κB to cerebral vasospasm after experimental subarachnoid hemorrhage in rabbits. *J Cereb Blood Flow Metab* **27:**1583–1592.

**Address correspondence to:** Dr. David S. Warner, Box 3094, Department of Anesthesiology, Duke University Medical Center, Durham, NC 27710. E-mail: david.warner@duke.edu